

822. Non-iterative mode shape expansion for three-dimensional structures based on coordinate decomposition

Fushun Liu¹, Zhengshou Chen², Wei Li³

¹Department of Ocean Engineering, Ocean University of China, Qingdao, 266100, China

²Department of Naval Architecture and Civil Engineering, Zhejiang Ocean University, Zhoushan, China

³Hydro China Huadong Engineering Corporation, Hangzhou, 310014, China

E-mail: ¹percyluu@ouc.edu.cn, ²aaaczs@163.com, ³weili018@163.com

(Received 10 April 2012; accepted 4 September 2012)

Abstract. The direct mode shape expansion method is an iterative technique, one can conclude that the convergence performance maybe challenged when applied to three-dimensional structures. In addition, mode shape values at different DOFs (degrees-of-freedom) sometimes are not in a same order of magnitude, which will produce much error for the estimation of small values of unmeasured mode components. Therefore this paper proposed a non-iterative mode shape expansion method based on coordinate decomposition technique. The advantage of coordinate decomposition is that the unmeasured components of mode shape values could be estimated with different weighting coefficients, even in a physical meaningful interval. Numerical studies in this paper are conducted for a 30-DOF cantilever beam with multiple damaged elements, as the measured modes are synthesized from finite element models. The numerical results show that the approach can estimate unmeasured mode shape values at translational and rotational DOFs in x , y and z directions with different weighting coefficients, respectively; and better mode shape expansion results can be obtained when proper constraints are employed. A numerical three dimensional structure is also investigated, and results indicate that the estimation of unmeasured components can be improved by imposing reasonable constraints based on the coordinate decomposition technique, even only translational DOFs of two diagonal nodes of the first floor are measured.

Keywords: non-iterative, direct mode shape expansion, three-dimensional structure, coordinate decomposition.

Introduction

For model updating and damage detection of structures [1-2], modal parameters such as frequencies and mode shapes are often required based on a limited number of sensors assembled at the joints of the structure. However, compared with the number of DOFs (degrees-of-freedom) of the corresponding finite element model, the number of sensors is less than the DOFs of the finite element model, which will cause spatial incompleteness of measured mode shapes.

To deal with incompleteness of measured mode shapes, Guyan [3] and Irons [4] firstly reported reduction method, in which the mass and stiffness matrices are partitioned into a set of master and slave DOFs. This method neglects the inertial term thus the higher mode shapes are mainly influenced, it only approximates the eigen analysis of the full system, and the results depend upon the type and number of master DOFs. Many attempts have been made to improve the accuracy of the static condensation by employing model-reduction transformation matrix to expand the measured spatially incomplete modes, such as the work by Kidder [5] and Miller [6], Michael and Ephrahim [7], which require proper selection of master DOFs. The System-Equivalent-Reduction Expansion Process (SEREP) method [8] utilizes the analytical mode shapes to generate a transformation matrix between the measured DOFs and the unmeasured DOFs. The SEREP method may produce poor expansion estimates if the experimental mode shapes are not well correlated with the corresponding analytical mode shapes, which often happens in cases with large modelling errors in the analytical model. In addition, the penalty

method [9] uses a weighting variable as a measure of the relative confidence in the experimental mode shapes to produce mode-expansion estimates by minimising the modal strain energies. Recently, Chen [10] proposed a new approach for expanding incomplete experimental mode shapes which considers the modelling errors in the analytical model and the uncertainties in the vibrational-mode data measurements. This method expresses the mode shapes of the tested structure as a linear combination of the independent analytical eigenvectors using a mass normalisation of the analytical eigenvectors and also the expansion of mode shapes by obtaining a general transformation matrix. Liu [11] presented a direct estimation method for expanding incomplete experimental mode shapes. The performance of the method was investigated using a 5 DOFs mass-spring system and a steel cantilever-beam experiment. Because iterations are needed for solving modelling errors in each step, we can conclude that it maybe computationally expensive for three dimensional structures. Liu [12] presented a rapid mode shape expansion method without considering the modeling errors. In this method, no constraints are imposed and numerical studies also indicate the estimation of unmeasured components of mode shapes will be influenced when modeling errors exceed the limitation of the method.

Considering mode shape values at different DOFs sometimes are not in a same order of magnitude, which will produce much error for the estimation of small values of unmeasured mode components, e.g., the first mode shape of a monosymmetrical structure dominantly vibrates in one translational direction, which means mode shape values at other translational directions are very small. Therefore, if the unmeasured components of mode shapes are decomposed and estimated with different weighting coefficients, mode shape expansion results may be improved. In this study, a non-iterative mode shape expansion method is presented by decomposing unmeasured mode shape components corresponding to different coordinates. The synthesised measurements of a numerical cantilever beam and a three dimensional platform are used to illustrate the procedure and demonstrate the performance of the proposed scheme, respectively.

Mode shape expansion based on coordinate decomposition

Similar to the work by Liu [11], we also define a hybrid vector for the j th mode, which includes the measured data at master coordinates and constant values at slave coordinates, i.e.:

$$\Phi'_j = [\text{measured} \quad \text{measured} \quad \cdots \quad \text{constant} \quad \text{constant} \quad \cdots \quad \text{constant}]^T \quad (1)$$

where superscript “ T ” is the transpose operator. For estimating the unmeasured mode shape values corresponding to different coordinates, we assume that the j th measured mode Φ'_j is a modification of Φ'_j by:

$$\Phi^*_j = \Phi'_j + \sum_{sxt=1}^{N_{sdoftx}} \delta_{sxt} \Phi'_{sxt,j} + \sum_{syt=1}^{N_{sdofty}} \delta_{syt} \Phi'_{syt,j} + \sum_{szt=1}^{N_{sdoftz}} \delta_{szt} \Phi'_{szt,j} + \sum_{sxr=1}^{N_{sdofrx}} \delta_{sxr} \Phi'_{sxr,j} + \sum_{syr=1}^{N_{sdofry}} \delta_{syr} \Phi'_{syr,j} + \sum_{s zr=1}^{N_{sdofrz}} \delta_{s zr} \Phi'_{s zr,j} \quad (2)$$

where $\Phi'_{sxt,j}$, $\Phi'_{syt,j}$ and $\Phi'_{szt,j}$ are modes which only have nonzero values at the s th translational DOFs in x , y and z directions respectively; N_{sdoftx} , N_{sdofty} and N_{sdoftz} are numbers of unmeasured translational DOFs in x , y and z directions respectively; and δ_{sxt} , δ_{syt} and δ_{szt} are mode-correction factors to be determined at translational DOFs in x , y and z directions. Likewise, $\Phi'_{sxr,j}$, $\Phi'_{syr,j}$ and $\Phi'_{s zr,j}$ are modes, N_{sdofrx} , N_{sdofry} and N_{sdofrz} are unmeasured

numbers, and δ_{sxt}^* , δ_{syt}^* and δ_{szt}^* are mode-correction factors corresponding to the s th rotational DOFs in x , y and z directions, respectively.

The stiffness and mass matrix of the actual (experimental) model is denoted by \mathbf{K}^* and \mathbf{M}^* , respectively. Then the relation for the j th eigenvalues and eigenvectors associated with \mathbf{K}^* and \mathbf{M}^* can be expressed as:

$$\mathbf{K}^* \Phi_j^* = \lambda_j^* \mathbf{M}^* \Phi_j^* \quad (3)$$

Here, we neglect modelling errors of the finite element model, i.e., choose:

$$\mathbf{K}^* = \mathbf{K} \quad (4)$$

and

$$\mathbf{M}^* = \mathbf{M} \quad (5)$$

In the following development, it is assumed that few of λ_j^* and Φ_j^* values are known measurements available from modal testing. Pre-multiplying Eq. (3) by Φ_i^T yields:

$$\Phi_i^T \mathbf{K}^* \Phi_j^* = \lambda_j^* \Phi_i^T \mathbf{M}^* \Phi_j^* \quad (6)$$

Substituting Eqs. (2), (4) and (5) into the above equation yields:

$$\Phi_i^T \mathbf{K}^* \left(\Phi_j^* + \sum_{sxt=1}^{N_{sdofxt}} \delta_{sxt}^* \Phi'_{sxt,j} + \sum_{syt=1}^{N_{sdofyt}} \delta_{syt}^* \Phi'_{syt,j} + \sum_{szt=1}^{N_{sdofzt}} \delta_{szt}^* \Phi'_{szt,j} + \sum_{sxr=1}^{N_{sdofxr}} \delta_{sxr}^* \Phi'_{sxr,j} + \sum_{syr=1}^{N_{sdofyr}} \delta_{syr}^* \Phi'_{syr,j} + \sum_{s zr=1}^{N_{sdofzr}} \delta_{s zr}^* \Phi'_{s zr,j} \right) = \quad (7)$$

$$\lambda_j^* \Phi_i^T \mathbf{M}^* \left(\Phi_j^* + \sum_{sxt=1}^{N_{sdofxt}} \delta_{sxt}^* \Phi'_{sxt,j} + \sum_{syt=1}^{N_{sdofyt}} \delta_{syt}^* \Phi'_{syt,j} + \sum_{szt=1}^{N_{sdofzt}} \delta_{szt}^* \Phi'_{szt,j} + \sum_{sxr=1}^{N_{sdofxr}} \delta_{sxr}^* \Phi'_{sxr,j} + \sum_{syr=1}^{N_{sdofyr}} \delta_{syr}^* \Phi'_{syr,j} + \sum_{s zr=1}^{N_{sdofzr}} \delta_{s zr}^* \Phi'_{s zr,j} \right)$$

Rearranging Eq. (7) and obtains:

$$\sum_{sxt=1}^{N_{sdofxt}} \delta_{sxt}^* \Phi_i^T (\mathbf{K}^* - \lambda_j^* \mathbf{M}^*) \Phi'_{sxt,j} + \sum_{syt=1}^{N_{sdofyt}} \delta_{syt}^* \Phi_i^T (\mathbf{K}^* - \lambda_j^* \mathbf{M}^*) \Phi'_{syt,j} + \sum_{szt=1}^{N_{sdofzt}} \delta_{szt}^* \Phi_i^T (\mathbf{K}^* - \lambda_j^* \mathbf{M}^*) \Phi'_{szt,j} + \sum_{sxr=1}^{N_{sdofxr}} \delta_{sxr}^* \Phi_i^T (\mathbf{K}^* - \lambda_j^* \mathbf{M}^*) \Phi'_{sxr,j} + \sum_{syr=1}^{N_{sdofyr}} \delta_{syr}^* \Phi_i^T (\mathbf{K}^* - \lambda_j^* \mathbf{M}^*) \Phi'_{syr,j} + \sum_{s zr=1}^{N_{sdofzr}} \delta_{s zr}^* \Phi_i^T (\mathbf{K}^* - \lambda_j^* \mathbf{M}^*) \Phi'_{s zr,j} - \Phi_i^T (\mathbf{K}^* - \lambda_j^* \mathbf{M}^*) \Phi_j^* = \quad (8)$$

For clarity, using a new symbol H to simplify the above equation, yields:

$$\sum_{sxt=1}^{N_{sdofxt}} \delta_{sxt}^* H_{sxt,ij} + \sum_{syt=1}^{N_{sdofyt}} \delta_{syt}^* H_{syt,ij} + \sum_{szt=1}^{N_{sdofzt}} \delta_{szt}^* H_{szt,ij} + \sum_{sxr=1}^{N_{sdofxr}} \delta_{sxr}^* H_{sxr,ij} + \sum_{syr=1}^{N_{sdofyr}} \delta_{syr}^* H_{syr,ij} + \sum_{s zr=1}^{N_{sdofzr}} \delta_{s zr}^* H_{s zr,ij} = -H_{ms,ij} \quad (9)$$

where $H_{sxt,ij} = \Phi_i^T (\mathbf{K}^* - \lambda_j^* \mathbf{M}^*) \Phi'_{sxt,j}$, $H_{syt,ij} = \Phi_i^T (\mathbf{K}^* - \lambda_j^* \mathbf{M}^*) \Phi'_{syt,j}$, $H_{szt,ij} = \Phi_i^T (\mathbf{K}^* - \lambda_j^* \mathbf{M}^*) \Phi'_{szt,j}$, and $H_{sxr,ij} = \Phi_i^T (\mathbf{K}^* - \lambda_j^* \mathbf{M}^*) \Phi'_{sxr,j}$, $H_{syr,ij} = \Phi_i^T (\mathbf{K}^* - \lambda_j^* \mathbf{M}^*) \Phi'_{syr,j}$, $H_{s zr,ij} = \Phi_i^T (\mathbf{K}^* - \lambda_j^* \mathbf{M}^*) \Phi'_{s zr,j}$.

In addition, a new index m is used to replace ij , Eq. (9) becomes:

$$\sum_{sxt=1}^{N_{sdoft}} \delta_{sxt} H_{sxt,m} + \sum_{syt=1}^{N_{sdoft}} \delta_{syt} H_{syt,m} + \sum_{szt=1}^{N_{sdoft}} \delta_{szt} H_{szt,m} + \sum_{sxr=1}^{N_{sdoft}} \delta_{sxr} H_{sxr,m} + \sum_{syr=1}^{N_{sdoft}} \delta_{syr} H_{syr,m} + \sum_{s zr=1}^{N_{sdoft}} \delta_{s zr} H_{s zr,m} = -H_{ms,m} \quad (10)$$

Eq. (10) can be rewritten in a matrix form, i.e.:

$$\begin{bmatrix} \mathbf{H}_{sxt} & \mathbf{H}_{syt} & \mathbf{H}_{szt} & \mathbf{H}_{sxr} & \mathbf{H}_{syr} & \mathbf{H}_{s zr} \end{bmatrix} \begin{Bmatrix} \delta_{sxt} \\ \delta_{syt} \\ \delta_{szt} \\ \delta_{sxr} \\ \delta_{syr} \\ \delta_{s zr} \end{Bmatrix} = \mathbf{H}_{ms} \quad (11)$$

One can rewrite Eq. (11) as:

$$\mathbf{G}^\ominus \Delta = \mathbf{F}^\ominus \quad (12)$$

where:

$$\mathbf{G}^\ominus = \begin{bmatrix} \mathbf{H}_{sxt} & \mathbf{H}_{syt} & \mathbf{H}_{szt} & \mathbf{H}_{sxr} & \mathbf{H}_{syr} & \mathbf{H}_{s zr} \end{bmatrix} \quad (13)$$

$$\Delta = \left\{ \delta_{sxt} \quad \delta_{syt} \quad \delta_{szt} \quad \delta_{sxr} \quad \delta_{syr} \quad \delta_{s zr} \right\}^T \quad (14)$$

$$\mathbf{F}^\ominus = \mathbf{H}_{ms} \quad (15)$$

Analytically, one can solve Δ in Eq. (12) by a standard inverse operation, $\Delta = (\mathbf{G}^\ominus)^{-1} \mathbf{F}^\ominus$ if \mathbf{G}^\ominus is a non-singular square matrix. For a non-square matrix \mathbf{G}^\ominus where the number of equations does not equal the number of unknowns, the equivalent operator is the pseudo-inverse. If \mathbf{G}^\ominus has more rows than columns, an over-determined case where there are more equations than unknowns, the pseudo-inverse is defined as:

$$\mathbf{G}^\# = \left((\mathbf{G}^\ominus)^T \mathbf{G}^\ominus \right)^{-1} (\mathbf{G}^\ominus)^T \quad (16)$$

for nonsingular $\left((\mathbf{G}^\ominus)^T \mathbf{G}^\ominus \right)$. The resulting solution $\Delta = \mathbf{G}^\# \mathbf{F}^\ominus$ is optimal in a least squares sense.

In this paper, we will employ Matlab function *lsqlin* to solve Eq. (12), i.e.:

$$\Delta = \text{lsqlin}(\mathbf{G}^\ominus, \mathbf{F}^\ominus, \mathbf{A}, \mathbf{b}, \text{Aeq}, \text{beq}, \text{LB}, \text{UB}) \quad (17)$$

Eq. (17) defines a set of lower and upper bounds on the design variables subject to $\mathbf{A} \times \Delta \leq \mathbf{b}$ and $\text{Aeq} \times \Delta = \text{beq}$, and the solution is in the range $\text{LB} \leq \Delta \leq \text{UB}$. Use empty matrices for LB and UB if no bounds exist.

Numerical study I: a cantilever beam

Similar to reference [11], we also use a cantilever beam to demonstrate the performance of

the improved method in this paper, as shown in Fig. 1, where each element is modeled as a uniform beam element, and each node has 3 DOFs. The analytical model and the measured modal information are generated from finite element models, with different sets of system coefficients. It is assumed that the analytical model is with a “wrong” set of coefficients (\mathbf{K} and \mathbf{M}), and the measured modal information is simulated from the finite element model with “right” coefficients (\mathbf{K}^* and \mathbf{M}^*). The beam is of length 3 m, breadth 25 cm and thickness 20 cm. Young’s modulus is taken as 3.2×10^{10} Pa, and mass density 2500 kg/m^3 (or mass density per unit length 125 kg/m). The cross section area and the associated moment of inertia are 0.05 m^2 and $1.66 \times 10^{-4} \text{ m}^4$, respectively.

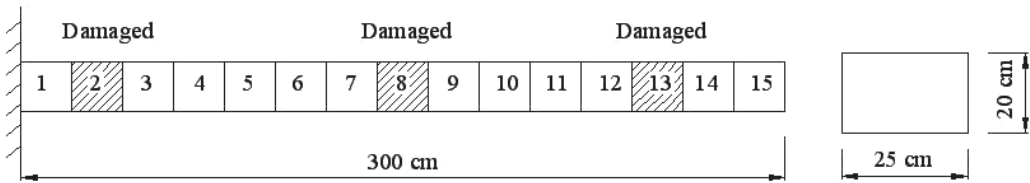


Fig. 1. Sketch of a 15-element cantilever beam

The true model is considered to be a damaged cantilever beam with multiple damages. The damages are modeled as the reduction in stiffness at elements 2, 8 and 13 by 35 %, 25 % and 55 %, respectively, from the analytical model, that is $\alpha_2 = -0.35$, $\alpha_8 = -0.25$ and $\alpha_{13} = -0.55$, where α_n represents the stiffness reduction of the n th element, and $n = 1, 2, \dots, 15$. In addition to the above α values at those damaged elements, the parameters of the true model are considered to be slightly different from those of the analytical model for other elements as well. Specifically, other elements of the true model are produced with the quantities α_n are generated based on the absolute value of the Gaussian distribution with mean 0 and standard deviation 0.35.

Theoretically, using \mathbf{K} to replace \mathbf{K}^* in Eq. (6) will produce unexpected errors, even wrong results may be caused when the difference between \mathbf{K} and \mathbf{K}^* is very obvious. Therefore, we firstly assume the stiffness \mathbf{K}^* is known, and all the translational DOFs can be measured, i.e., there are 15 master DOFs and 30 slave DOFs, thus the hybrid vector can be constructed based on Eq. (7), in which all the constant values are assumed to be one. If we use 45 modes from the analytical model, then 45 equations will be formed in the light of Eq. (16) for each measured mode, which are sufficient to solve 30 unknowns. Shown in Fig. 2(a) is the comparison of the first mode shape values corresponding to axial translational DOFs, plotted against the degrees of freedoms, and mode shape values corresponding to rotational DOFs are plotted in Fig. 2(b). From Fig. 2, one can find that the unmeasured components of the first mode shape are estimated properly without the modeling errors.

Indeed, modeling errors between the finite element model and the tested structure exist in most situations, especially when model updating techniques are not employed. Therefore, the following work is to investigate the feasibility of the proposed method when modeling errors are neglected. Here, given the same consideration, we also assume only 15 translational DOFs are measured, except that neglecting the modeling errors between the finite element model and the tested structure, i.e., using \mathbf{K} to replace \mathbf{K}^* in Eq. (6). Fig. 3 to Fig. 5 is the first three mode shape values comparison at the unmeasured translational and rotational DOFs, respectively. One concludes that the unmeasured components of mode shapes are estimated reasonably with the modeling errors when implementing the proposed approach.

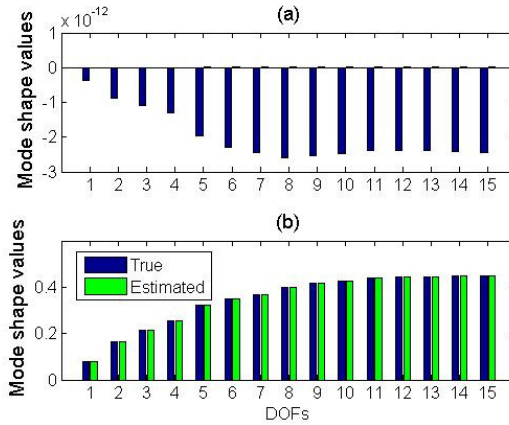


Fig. 2. The first mode shape expansion when the stiffness of the tested structure is known: (a) For translational DOFs; and (b) For rotational DOFs

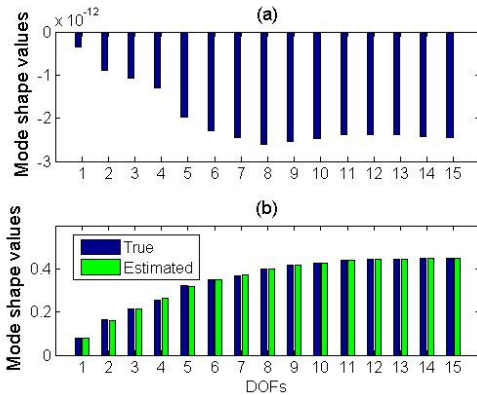


Fig. 3. The first mode shape expansion with modeling errors: (a) For translational DOFs; and (b) For rotational DOFs

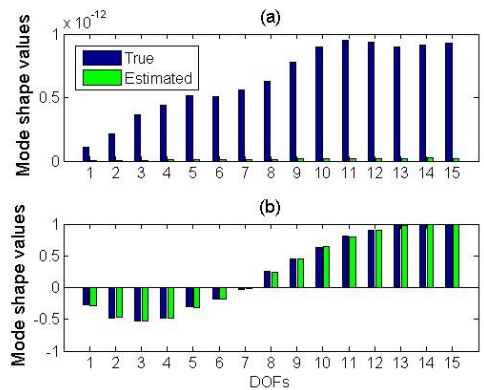


Fig. 4. The second mode shape expansion with modeling errors: (a) For translational DOFs; and (b) For rotational DOFs

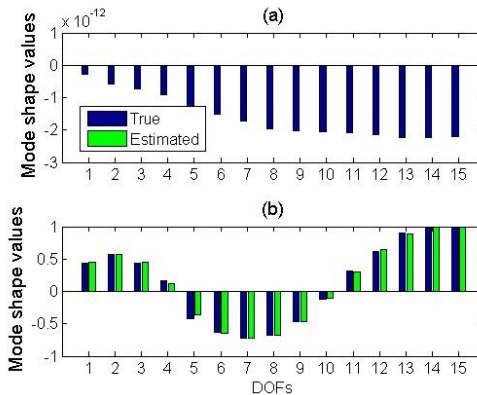


Fig. 5. The third mode shape expansion with modeling errors: (a) For translational DOFs; and (b) For rotational DOFs

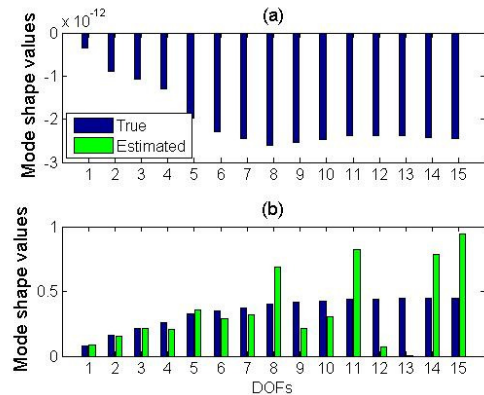


Fig. 6. The first mode shape expansion with a 5 % corruption level without constraints imposed: (a) For translational DOFs; and (b) For rotational DOFs

Note that Fig. 2 to Fig. 5 are results obtained from noise free measurements. In practice, modal measurements always contain errors. The remaining numerical study focuses on implementing the proposed method when corrupted modes are used. The value of the corrupted mode at each measured DOF will be generated by multiplying its true value by a factor $(1 + \varepsilon)$, where ε is simulated based on a Gaussian distribution with mean 0 and a specified standard deviation that equals the corruption (noise) level. Based on the same considerations yields Fig. 2, except that all translational DOFs of the beam are measured under a 5 % corruption level, one obtains Fig. 6. Fig. 6 shows the estimation results of the first modes. Fig. 6 clearly exhibit that noise has an obvious influence on the mode shape estimation at rotational DOFs, such as at nodes 8 to 15.

Considering the fact that the unmeasured components of the mode shape have been decomposed into three groups for two dimensional structures, i.e., mode shape values corresponding to translational DOFs in x and y directions, and ones corresponding to rotational DOFs. Thus, we can estimate the three groups with different weighting coefficients. Based on the same considerations yields Fig. 7, except that the constraints are imposed, i.e., mode-correction factors for axial translational DOFs very close to zero, and mode-correction factors at rotational DOFs for node 8 to 15 are limited in the interval from -0.6 to -0.4, which can be concluded from the characteristics of the first mode of finite element model, other mode-correction factors are permitted in all real number field. Compare Fig. 7 to Fig. 6, one concludes that the estimation of unmeasured mode shape components can be improved when proper constraints are employed, which will be more important for three dimensional structures.

Numerical study II: a three dimensional structure

A more real structure, i.e., one three dimensional offshore platform is investigated too, as shown in Fig. 8. It consists of 36 steel tubular members: 4 legs dispersed into 12 members, with uniform outer diameter 120 cm and wall thickness 2.8 cm; other 24 members with 70 cm and 2.2 cm. The heights of three stories, from first to third, are 8.5 m, 8.5 m, and 6.5 m, respectively. Side lengths at the top are 11.52 m, 8.52 m, 11.52 m, and 8.52 m, respectively, and the 4 legs are fixed at the ground. Young’s modulus is taken as 2.1×10^{11} Pa, Poissons ratio 0.3, and mass density 7850 Kg/m^3 . Using the finite-element method and performing an eigenvector analysis yields a structure that has the following first five modal frequencies: 8.95, 9.07, 11.14, 11.81 and 19.11 Hz. In this study, the true model is considered to be a damaged platform. The damage is modeled as a reduction in the stiffness of element 4, 22 and 25 by 30 %, 20 % and 50 % from the analytical model, respectively.

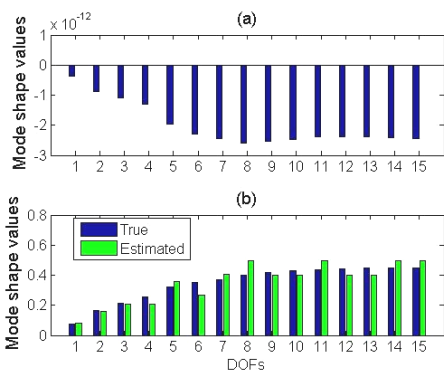


Fig. 7. The first mode shape expansion with a 0.5 % corruption level with constraints imposed

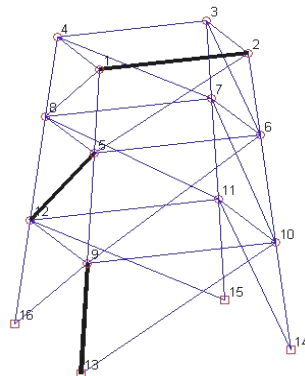


Fig. 8. A three dimensional structure

Firstly, we study the feasibility neglecting the difference between \mathbf{K} and \mathbf{K}^* on the estimation of unmeasured mode components. Assume translational DOFs in x , y and z directions at nodes 1 to 8 are measured (i.e., there are 48 master DOFs and 48 slave DOFs). Thus, the hybrid vector can be constructed based on Eq. (7), in which all of the constant values are assumed to be one. If we use 72 modes from the analytical model, then 72 equations will be assumed in the light of Eq. (12) for each measured mode, which are sufficient to solve 48 unknowns. Shown in Fig. 9 is the comparison of the first mode shape values corresponding to translational DOFs, plotted against the degrees of freedoms, and mode shape values corresponding to rotational DOFs are plotted in Fig. 10. From Fig. 9 and Fig. 10, one can find that the unmeasured components of the first mode shape are estimated properly without the modeling errors.

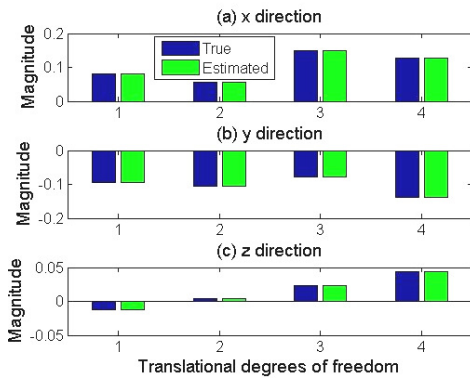


Fig. 9. Mode shape at translational DOFs when constraints are imposed, in (a) x direction, (b) y direction, and (c) z direction

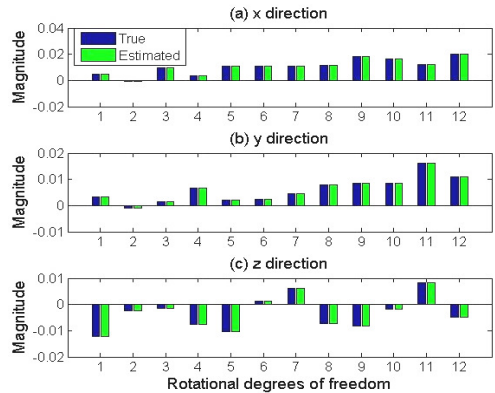


Fig. 10. Mode shape at rotational DOFs when constraints are imposed, in (a) x direction, (b) y direction, and (c) z direction

When the difference between \mathbf{K} and \mathbf{K}^* exists, the estimation of unmeasured mode components will be influenced. Here, we also assume translational DOFs in x , y and z directions at nodes 1 to 8 are measured, and 72 modes from the finite element model are used too. Fig. 11 and Fig. 12 show the comparison of the first mode shape values corresponding to translational and rotational DOFs, respectively. One concludes that translational unmeasured components could be estimated properly, while the estimation of rotational unmeasured components has more errors, such as values estimation in y rotational DOFs.

To improve the unmeasured components estimation, some constraints could be applied based on the decomposition of unmeasured components. For example, the second and the third estimated values in Fig. 12(c) should be less than zero. Based on the same considerations yields Fig. 12, one obtains Fig. 13. From Fig. 13, one can find that unmeasured components estimation could be improved if proper constraints are provided. The above initial estimating domain can be obtained based on the mode shape values of the FEM model at corresponding slave coordinates.

Conclusions

Direct mode shape expansion method is an iterative technique without requiring model-reduction transformation matrix compared with traditional expansion methods. Because of the fact that mode shape values at different DOFs sometimes are not in a same order of magnitude, which will produce much error for the estimation of small values of unmeasured mode components when these values are estimated in a same interval, a decomposition technique for

unmeasured components of mode shapes is employed, and a non-iterative mode shape expansion method is presented by decomposing unmeasured mode shape components corresponding to different coordinates. The synthesised measurements of a numerical cantilever beam are used to illustrate the performance of the proposed scheme, and the numerical results reveal that the estimation of unmeasured components of mode shapes will be improved utilizing the decomposition technique and the proper constraints are imposed. The numerical study of a platform demonstrated that the estimation of unmeasured components could be improved by imposing reasonable constraints based on coordinate decomposition technique, even only translational DOFs of two diagonal nodes are measured.

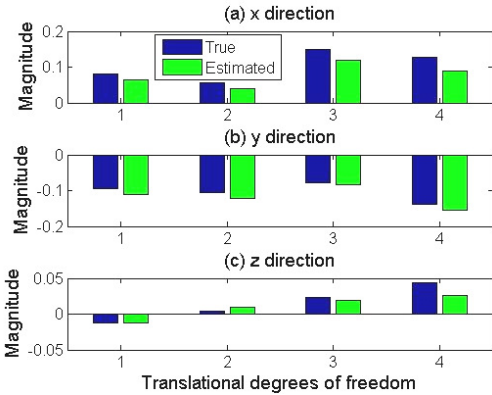


Fig. 11. Mode shape at translational DOFs when constraints are imposed, in (a) *x* direction, (b) *y* direction, and (c) *z* direction

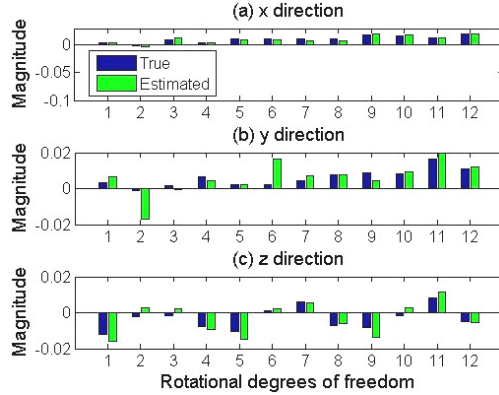


Fig. 12. Mode shape at rotational DOFs when constraints are imposed, in (a) *x* direction, (b) *y* direction, and (c) *z* direction

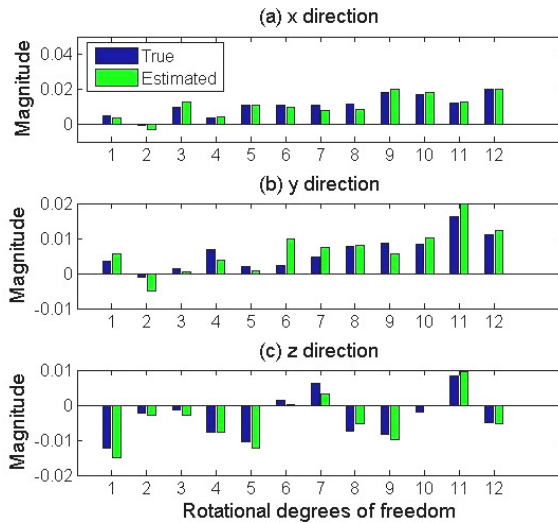


Fig. 13. Mode shape at rotational DOFs when constraints are imposed, in: (a) *x* direction, (b) *y* direction, and (c) *z* direction

Acknowledgements

The authors wish to acknowledge the financial support of the 973 project (Grant No. 2011CB013704), of the National Natural Science Foundation of China (Grant

No. 51009124), and of the Natural Science Foundation of Shandong Province (Grant No. ZR2009FQ007).

References

- [1] **Chen H. P., Bicanic N.** Inverse damage prediction in structures using nonlinear dynamic perturbation theory. *Computational Mechanics*, Vol. 37, Issue 5, 2006, p. 455–467.
- [2] **Li H. J., Liu F. S., Hu S.-L. J.** Employing incomplete complex modes for model updating and damage detection of damped structures. *Science in China Series E: Technologies*, Vol. 51, Issue 12, 2008, p. 2254–2268.
- [3] **Guyan R.** Reduction of stiffness and mass matrices. *AIAA Journal*, Vol. 3, Issue 2, 1965, p. 380.
- [4] **Irons B.** Structural eigenvalue problems: elimination of unwanted variables. *AIAA Journal*, Vol. 3, Issue 5, 1965, p. 961–962.
- [5] **Kidder R. L.** Reduction of structural frequency equations. *AIAA Journal*, Vol. 11, Issue 6, 1973, p. 892.
- [6] **Miller C. A.** Dynamic reduction of structural models. *Journal of the Structural Division*, Vol. 106, Issue 10, 1980, p. 2097–2108.
- [7] **Michael P., Ephraim G.** Improvement in model reduction schemes using the system equivalent reduction expansion process. *AIAA Journal*, Vol. 34, Issue 10, 1996, p. 2217–2219.
- [8] **O'Callahan J. C.** A procedure for an improved reduced system (IRS). *Seventh International Modal Analysis Conference*, Las Vegas, Nevada, USA, 1989, February.
- [9] **Levine-West M., Milman M., Kissil A.** Mode shape expansion techniques for prediction: experimental evaluation. *AIAA Journal*, Vol. 34, Issue 4, 1996, p. 821–829.
- [10] **Chen H. P.** Mode shape expansion using perturbed force approach. *Journal of Sound and Vibration*, Vol. 329, 2010, p. 1177–1190.
- [11] **Liu F. S.** Direct mode-shape expansion of a spatially incomplete measured mode by a hybrid-vector modification. *Journal of Sound and Vibration*, Vol. 330, Issue 18-19, 2011, p. 4633–4645.
- [12] **Liu F. S., Li H. J.** Rapid direct-mode shape expansion for offshore jacket structures using a hybrid vector. *Ocean Engineering*, Vol. 51, Issue 1, 2012, p. 119–128.